CMLS, Cell. Mol. Life Sci. 60 (2003) 198–211
1420-682X/03/010198-14

CMLS Cellular and Molecular Life Sciences

Research Article

Regulation of caldesmon activity by Cdc2 kinase plays an important role in maintaining membrane cortex integrity during cell division

Y. Li, D. Wessels, T. Wang, J. L-C. Lin, D. R. Soll and J. J-C. Lin*

Department of Biological Sciences, University of Iowa, 138 Biology Building, Iowa City, Iowa 52242-1324 (USA), Fax: +1 319 335 1069, e-mail: Jim-Lin@uiowa.edu

Received 4 September 2002; received after revision 25 November 2002; accepted 4 December 2002

Abstract. To study the mitosis-specific phosphorylation of caldesmon (CaD), we generated a mutant of the C-terminal fragment (amino acids 244–538) of human fibroblast CaD (CaD39-6F), as well as a mutant of the full-length CaD (CaD-6F), in which all six potential phosphorylation sites for Cdc2 kinase were abolished. The mitotic CaD39-6F-overexpressing cells required more time to progress from anaphase start to 50% cytokinesis, exhibited larger size, and abnormally formed numerous small blebs. In contrast, overexpression of the wild-type C-terminal fragment of CaD (CaD39) did not result in abnormal bleb formation, but led to larger size and prolonged the time requirement between anaphase start and 50% cytokinesis. Similar abnormal blebs were also observed in the CaD-6F-overexpressing cells. CaD-6F-overexpressing cells did not show larger size but required more time to progress from anaphase start to 50% cytokinesis. These results suggest that mitosis-specific phosphorylation of CaD plays a role in inhibiting bleb formation and that the N-terminal fragment of CaD is required for cell size determination.

Key words. Mitosis-specific phosphorylation; phosphorylation-defective mutant; blebbing; 2D and 3D dynamic image analysis; microfilament; cytokinesis.

Caldesmon (CaD) is a myosin-, actin-, tropomyosin-, and Ca^{2+}/calmodulin-binding protein implicated in the control of microfilament activity and organization in both smooth muscle and non-muscle cells [1–5]. In vitro it exhibits a potent inhibitory effect on actin-tropomyosin-activated myosin ATPase and actin filament motility. Furthermore, CaD is able to stimulate polymerization of microfilaments [6] and the assembly of soluble myosin into filaments [7]. Finally, CaD has either an antagonistic or synergistic effect on other actin-binding proteins. On the one hand, it stimulates the binding of tropomyosin to actin filaments [8, 9]. On the other, together with tropomyosin, CaD impairs the actin-severing activity of gelsolin [10, 11] and the actin binding of fascin [12]. Consistent with the in vitro observations, in vivo studies also suggest a role for CaD in regulating both the contraction force of the actomyosin system and the stabilization of microfilaments. Microinjection of an antisense oligo specific to CaD led to an increase in the interaction of actomyosin cross-bridge cycling in vascular smooth muscle [13]. Transient expression of full-length CaD resulted in the formation of thick stress fibers in Chinese Hamster Ovary (CHO) cells [14], suggesting that CaD stabilizes actin filaments. However, a contradictory observation was reported that transient transfection of CaD in human fibroblasts interfered with stress fiber formation [15]. The discrepancy in these results may arise from the in-

* Corresponding author.

trinsic nature of transient expression, such as heterogeneity of expression levels and unstable phenotypes associated with a transient robust increase of the exogenous protein. To address this problem, our laboratory previously adopted a stable overexpression system. We reported that forced expression of the C-terminal half [amino acids (aa) 244–538] of human fibroblast CaD, termed CaD39, in CHO cells stabilized endogenous tropomyosin and microfilaments [16] and enhanced early cell attachment and spreading [17]. However, these phenotypes were not observed in the stable clones overexpressing either the N-terminal fragment or full-length CaD, suggesting that the C-terminal fragment, CaD39, can act as a dominant-negative mutant to interfere with the normal regulation and function of CaD in vivo.

The effects of CaD on microfilaments can be reversed by the addition of an excess of Ca^{2+}/calmodulin [2, 4, 5, 18–22] or by phosphorylation by Cdc2 kinase [12, 23–26], both of which are thought to be critical for regulating the organization and dynamics of the cytoskeleton. During mitosis, CaD is phosphorylated by Cdc2 kinase and dissociates from the actin filaments [24]. In the CaD39-overexpressing clones, we observed alleviation of CaD39-induced effects during mitosis, which coincided with CaD39 phosphorylation and its partial dissociation from the isolated microfilaments [17]. Therefore, phosphorylation of CaD and its subsequent dissociation from microfilaments seem, at least in part, responsible for regulating mitosis-specific reorganization of actin filaments. Further in vitro studies showed that recombinant CaD could be phosphorylated by Cdc2 kinase and resulted in dissociation of CaD from the actin filaments and a subsequent decrease in its inhibitory effect on myosin ATPase [23], suggesting a potential role for phosphorylation by Cdc2 in regulating CaD activity. However, despite these in vitro data, we still do not know whether Cdc2 kinase is solely responsible for the phosphorylation of CaD during cell division and whether the phosphorylation regulates the CaD activity in the same way as observed in the in vitro experiments. One approach to address these questions, and to further investigate the effects of CaD phosphorylation on the actin cytoskeleton rearrangement during mitosis, is to create dominant-negative mutants that cannot be regulated by Cdc2 kinase, stably express them in the cells, and study the mutant phenotypes. One could mutate the phosphorylation sites into aspartic acid so as to mimic the constitutively phosphorylated CaD. However, based on the in vitro data, such a mutant is unlikely to bind to actin filaments, and is thus unlikely to exert any dominant-negative effect on the organization of microfilaments. Therefore, one might not observe any mutant phenotype in such cells because the endogenous CaD could regulate the actin filaments as in wild-type cells. Instead, we created a CaD39 mutant, termed CaD39-6F, and a full-length CaD mutant, termed CaD-6F, in which all six putative Ser/Thr residues for Cdc2 kinase were mutated into Ala. We established several stable cell lines expressing either mutant protein. We report that the mutant CaD39-6F could not be phosphorylated and dissociated from the actin filaments during mitosis. Compared to the wild-type control cells, CaD39-6F-overexpressing cells took longer to progress from anaphase start to 50% cytokinesis, had a significantly bigger cell size, and exhibited abnormal blebs. Similar blebbing was also found in the cells overexpressing full-length mutant CaD-6F, suggesting a role for Cdc2 phosphorylation of CaD in regulating cortical tension and inhibiting bleb formation during cytokinesis. CaD-6F-overexpressing lines did not exhibit larger cells at mitosis, suggesting an additional regulatory mechanism at the N-terminal half of CaD.

Materials and methods

Construction of CaD39-6F mutants

Six consensus sites (Ser/Thr-Pro) for Cdc2 kinase phosphorylation were found to be located on the C-terminal fragment of CaD (CaD39). They are Thr^{383}, Ser^{469}, Thr^{475}, Thr^{489}, Ser^{504}, and Ser^{534}, which are highly conserved between human and rat CaD. Apart from Thr^{383}, all equivalent sites in the rat CaD were identified as the mitosis-specific phosphorylation sites [27]. Using six different primers corresponding to each site, six single mutants with changes from Ser/Thr to Ala were generated by site-directed mutagenesis from the cDNA of plasmid pET-CaD39 [8]. Site-directed mutagenesis was performed as described in the Clontech transformed site-directed mutagenesis kit (Clontech, Palo Alto, Calif.). The six target primers used for mutagenesis are the following sequences with mutated codon underlined.

$CaDT^{383}$: 5′ CCTTTAGGAGCGAAACACTTG 3′
$CaDS^{469}$: 5′ GCAGTGGGGGCTGAAAACAC 3′
$CaDT^{475}$: 5′ CTTATTTGGTGCGCCTGCTG 3′
$CaDT^{498}$: 5′ CCATCTGGGGCTTTAGTTAG 3′
$CaDS^{504}$: 5′ GGGAGCAGGTGCCTTGTTTC 3′
$CaDS^{534}$: 5′ CCTTAGTGGGGGCAGTGACC 3′

The selective ClaI primer (5′ CAGCTTATCAcCGATAAGCT 3′) was used for the selection of mutated circular DNA from the synthesized DNA mixture. This primer contains a base pair change within the unique ClaI site at position 24 of the pET8c/s vector. Similarly, two-site ($Ser^{469}Thr^{475}$, $Thr^{475}Ser^{504}$, and $Thr^{498}Ser^{504}$), three-site ($Thr^{383}Thr^{498}Ser^{504}$ and $Thr^{475}Thr^{498}Ser^{504}$), and five-site ($Thr^{383}Ser^{469}Thr^{475}Thr^{498}Ser^{504}$ and $Ser^{469}Thr^{475}Thr^{498}Ser^{504}Ser^{534}$) mutations were generated with respective mixture of target primers together with the ClaI selective primer in the synthesis step. To generate four-site ($Ser^{469}Thr^{475}Thr^{498}Ser^{504}$) and six-site mutations, three-site ($Thr^{475}Thr^{498}Ser^{504}$) and five-site ($Ser^{469}Thr^{475}Thr^{498}$

$Ser^{504}Ser^{534}$) mutated clones were further mutated at Ser^{469} and Thr^{383}, respectively, with the other selective primer. This selective primer (5′ AGGGAgAGCTTC-GACCGATG 3′) contains a base pair change within the unique SalI site at position 928 of the pET8c/s vector. The plasmid with the six-site mutant CaD39 was named pET-CaD39-6F. All mutant DNAs were sequenced by the dideoxy sequencing method using Sequenase (U.S. Biochemical Corp., Cleveland, Ohio). The plasmid encoding the full-length CaD lacking all six Cdc2 sites (called pETCaD-6F) was constructed by replacing the PvuI fragment of pETCaD with the mutated PvuI fragment from pETCaD39-6F, which contained all six mutated sites. For the purpose of eukaryotic expression, the XbaI fragments from pETCaD39-6F and pETCaD-6F were subcloned into the XbaI site of pCB6hx vector [16] and the resulting plasmids were called pCBCaD39-6F and pCBCaD-6F, respectively.

Cell transfection and immunofluorescence microscopy

CHO cells were cultured in Dubecco modified Eagle's medium (DMEM) plus 10% fetal bovine serum (FBS) and kept in a 37 °C humidified incubator with 5% CO_2. Plasmid DNAs were introduced into the cells using the liposome transfection reagent DOTAP (Boehringer Mannheim, Indianapolis, Ind.). For establishment of stable clones expressing CaD39-6F, CaD, or CaD-6F, cells at 1 day after transfection were selected in DMEM plus 10% FBS with 500 µg/ml G418 (GIBCO BRL, Gaithersburg, Md.). After 2 weeks of selection, single cells with different levels of expression were cloned, and expanded. The expression of CaD39-6F was tested using indirect immunofluorescent microscopy as described elsewhere [16]. The primary antibody used in this study was the anti-caldesmon monoclonal antibody C21 diluted 1 : 1000. C21 recognizes the C-terminal 10-kDa fragment of chichen gizzard CaD [28]. The sequences of this region are highly conserved among species. Therefore, the reactivities of C21 antibody to the endogenous CHO CaD and the exogenous human CaD are very similar. However, due to the overexpression of the exogenous proteins, C21 is able to strongly cross-react with CaD39 and barely detects endogenous CHO CaD when used at such high dilution [16]. The recognition of endogenous CaD requires a C21 antibody at ×100 dilution. The second antibody was FITC-conjugated goat anti-mouse IgG (Sigma, St. Louis, Mo.). Stable lines 39-6FC10, 39-6FC36, 39-6FC2, 39-6FC6, 39-6FC19, and 39-6FC33 were obtained expressing low to high amounts of CaD39-6F, respectively. The non-expressing but G418-resistant cell line 39-6FC5 was also isolated for use as a control. Similarly, stable line CaD-6FC10, CaD-6FC27, and CaD-6FC28, expressing low to high amounts of CaD-6F, were obtained and characterized. A previously isolated stable line 39C15 expressing wild-type CaD39 [16], as well as a stable line CaDC6, expressing wild-type full-length CaD, was also included in this study for comparison.

Urea/SDS-PAGE and Western blot analysis

Interphase 39-6FC33 cells and 39C15 [16] cells, which express CaD39-6F and CaD39, respectively, were rinsed three times in phosphate-buffered saline (PBS) and harvested in 2× SDS-PAGE gel sample buffer as described elsewhere [17]. Mitotic cells were collected after 4 h treatment of interphase cells with 0.25 µg/ml nocodazole (Sigma) by the shake-off method as described elsewhere [17]. Collected cells were then washed with PBS and dissolved in 2× SDS-PAGE gel sample buffer. Total proteins were resolved by 8% SDS-PAGE containing 6 M urea. After electrophoresis, proteins were transferred to nitrocellulose paper for Western blot analysis with either monoclonal antibody C21 or C57 as described elsewhere [17].

Protein expression and purification in bacteria

pETCaD39-6F and pETCaD39 were transformed into the bacterial strain BL21(DE3)pLysS. Expression of CaD39 and CaD39-6F proteins were induced as described previously [8]. The recombinant CaD39 and CaD39-6F proteins were purified as described previously [8], including heat treatment of bacterial lysate, ammonium sulfate fractionation, and two FPLC column chromatographies (Mono S column and Superose 12 column). The fractions containing recombinant proteins were identified by SDS-PAGE as described previously [8].

In vitro phosphorylation assay and actin-binding assay

For phosphorylation assay of CaD39/CaD39-6F, either 5 µM CaD39 or 10 µM CaD39-6F was incubated with 1.5 units Cdc2 kinase (New England BioLabs, Beverly, Mass.) in the kinase buffer containing 10 mM imidazole buffer, pH 7.0, 30 mM NaCl, 1 mM NaF, and 100 µM γ-^{32}P ATP (5 µC/µl) at 30 °C. At different time intervals, 5 µl each of sample was collected and the reaction terminated by addition of an equal volume of 2× SDS-PAGE gel sample buffer containing 10 mM NaF. The levels of ^{32}P incorporation into CaD39 and CaD39-6F were then analyzed by SDS-PAGE followed by autoradiography. In the competition assay for Cdc2 kinase activity, variable concentrations of CaD39-6F (0, 0.025, 0.25, 1.25, 2.5, and 5 µM) were added into the reaction mixture containing 5 µM histone H1, 1.5 units Cdc2 kinase, 100 µM γ-^{32}P-ATP (5 µC/µl). After 60 min incubation at 30 °C, the reactions were terminated by the addition of 2× gel sample buffer and analyzed by SDS-PAGE and autoradiography.

The actin-binding assay was based on a cosedimentation method [29] and performed on a Beckman airfuge rotor A-100/18 as described previously [8].

Microfilament isolation

Tropomyosin-enriched microfilaments were isolated from interphase and mitotic 39-6FC33 cells as described previously [17, 30]. Interphase cells from 20 culture dishes (100 mm) or the collection of mitotic cells from 40 dishes (150 mm) were extracted in KTG solution (0.05% Triton X-100, 0.1 M PIPES, 5 mM $MgCl_2$, 0.2 mM EGTA, 4 M glycerol), and the cytoskeletal residues homogenized in the presence of 5 mM ATP. After centrifugation, the supernatant was incubated with a 1/10 volume of an anti-tropomyosin monoclonal antibody to precipitate microfilaments. The aggregated microfilaments were collected by low-speed centrifugation and analyzed by Western blot analysis.

2D-DIAS analysis of mitotic cells expressing CaD39-6F

Cell dynamics during mitosis were analyzed using the 2D-DIAS program [31–33] as previously described [17, 34]. Briefly, a coverslip on which cells were grown was transferred to a Dvorak-Stotler perfusion chamber (Lucas-Highland, Chantilly, Va.) positioned on a microscope stage prewarmed to 35 °C. Mitotic cells were video-recorded via a 63× DIC objective on a Zeiss ICM405 inverted microscope equipped with an Optronics cooled CCD camera (Optronics, Galito, Calif.). The recorded images were digitized at a rate of 3.75 frames per minute onto the hard disk of a Macintosh G4 computer (Apple Computer, Cupertino, Calif.) equipped with a Data Translation frame grabber board (Data Translation, Marlboro, Mass.) and 2D-DIAS software [31–33]. Cell outlines were traced manually. Methods for computing parameters derived from 2D-DIAS have been presented elsewhere [31, 32].

3D reconstruction and motion analysis of dividing cells

For 3D reconstruction, the methods of Wessels et al. [35] were employed. In brief, cells were positioned on the stage of a Zeiss Axioplan 2 microscope equipped with DIC optics and a 63× planapo objective. The coarse-focus knob of the microscope was connected to a computer-regulated microstepper motor programmed to move the focus from the substratum through 25 µm in the z-axis in 2 s. Images were acquired with an Optronics cooled CCD camera, recorded onto videotape and subsequently entered into a Macintosh G4 computer equipped with a data translation frame grabber capable of acquiring images at a rate of 30 frames per second with Adobe Premiere software. Sixty optical sections were acquired at 0.4-µm increments in the z-axis over a 2-s period for each reconstruction, and repeated at 4-s intervals. The optical sections were traced, stacked, and converted to a faceted image with 3D-DIAS software as previously described [31–35].

Results

Forced expression of CaD39-6F or CaD-6F in CHO cells

To examine the effects of CaD phosphorylation by Cdc2, site-directed mutagenesis was used to generate the mutants of C-terminal fragment and full-length human fibroblast CaD (termed CaD39-6F and CaD-6F, respectively), in which all six putative Ser/Thr phosphorylation sites were substituted with Ala. Several independent stable clones expressing either CaD39-6F or CaD-6F were obtained. As shown in figure 1, three of the CaD39-6F-overexpressing clones (C6, C19, and C33) expressed high levels of the exogenous protein, while one clone (C5) had no detectable expression. The expression levels of CaD39-6F in each stable clone remained unchanged over passages. The amount of CaD39-6F expressed in the clone 39-6FC33 was comparable to that of CaD39 expressed in the previously isolated CaD39-expressing clone 39C15 (data not shown), in which the molar ratio of the exogenous CaD39 to the endogenous CaD protein is about 80 [16]. The overexpressing clones 39-6FC33 and 39-6FC19 were used in this study for subsequent functional analyses, while the non-expressing, G418-resistant clone 39-6FC5 was included as a negative control. As shown in figure 2, three stable clones (CaD-6FC10, CaD-6FC27, and CaD-6FC28) overexpressing full-length CaD defective at all six phosphorylation sites were obtained. The CaD-6F expression levels for both CaD-6FC10 and CaD-6FC27 were about 1.1 times that of endogenous CHO CaD (lanes 2 and 3 of fig. 2B), while clone CaD-6FC28 expressed about 5.2 times CHO CaD (lane 4 of fig. 2B). Figure 3 schematically diagrams the wild-type human fibroblast CaD and CaD39, as well as the mutant proteins CaD39-6F and CaD-6F. Also listed in figure 3

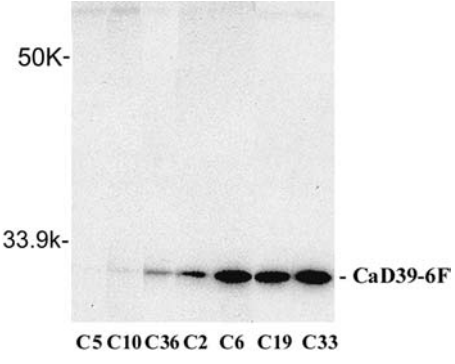

Figure 1. Western blot analysis of stable clones expressing CaD39-6F mutant protein. Total proteins were prepared from six stable lines (39-6FC10, C36, C2, C6, C19, and C33) expressing low to high levels of CaD39-6F mutant protein and a non-expressing control line 39-6FC5. Equal amounts of total proteins from each line were separated by SDS-PAGE and transferred to nitrocellulose paper for Western blot analysis with monoclonal anti-CaD antibody C21.

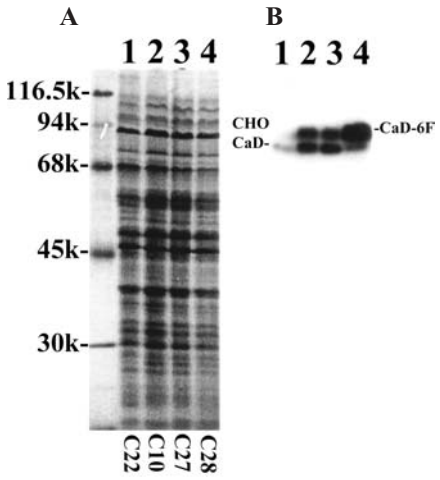

Figure 2. Western blot analysis of stable clones expressing CaD-6F mutant protein: (*A*) amido black-stained blot to show total protein loadings for the corresponding Western blots (*A*); Western blot analysis with monoclonal antibody C21 against CaD (*B*). Total protein extracts were prepared from stable line CaD-6FC10 (lane 2), CaD-6FC27 (lane 3), and CaD-6FC28 (lane 4), expressing medium to high levels of CaD-6F mutant protein, as well as a non-expressing line CaD-6FC22. Aliquots of total extracts were blotted with C21 (*B*). Both CaD-6FC10 and CaD-6FC27 expressed about the same amounts of mutant CaD-6F protein as endogenous CaD (CHO CaD), whereas the clone CaD-6FC28 expressed about 5.2 times higher than endogenous CaD (lane 4 in *B*).

are the stable cell lines used in this study that overexpress different constructs.

CaD39-6F mutant protein retains F-actin-binding ability

To detect the distribution of CaD39-6F in the overexpressing cell line, we used a highly diluted C21 (1000-fold dilution) in the immunofluorescence microscopy that could only detect the presence of overexpressed CaD39-6F [16]. Force-expressed CaD39-6F protein was able to assemble onto stress fibers (fig. 4A) and to localize to membrane ruffle regions (data not shown) at interphase. The distribution of CaD39-6F in interphase cells was very much like that of endogenous CaD (fig. 4F) or force-expressed CaD39 in CHO cells [16], suggesting that the mutation of phosphorylation sites for Cdc2 kinase did not affect overall actin-binding ability. Similar staining patterns were also observed in the CaD-6FC28 clone (data not shown). The retention of actin-binding ability for CaD39-6F mutant protein was further confirmed by the in vitro cosedimentation assays, in which recombinant CaD39 or CaD39-6F proteins were incubated with skeletal muscle F-actin in the presence or absences of tropomyosin. After centrifugation, comparable amounts of both CaD39 and CaD39-6F proteins were found in the pellet fractions, indicative of their bindings to F-actin (data not shown). Under this assay condition, there was no significant difference in their binding affinities even in the presence of tropomyosin (data not shown).

Although CaD39-6F retains the ability to bind to actin filaments, this association did not seem to be properly regulated during cell division. At early mitosis, the CaD39-6F proteins concentrated in the cell cortex as did F-actin (fig. 4B, C). During cytokinesis, some of the CaD39-6F mutant proteins were still localized in the cleavage furrow, but significant amounts remained in the cortex region, resulting in a much broader staining band of CaD39-6F (fig. 4D) than that of F-actin (fig. 4E). In contrast, the staining of normal CHO cells with C21 antibody at 1:100 dilution revealed a diffused distribution of the wild-type CaD at similar stages of mitosis (fig. 4G, I).

CaD39-6F cannot be phosphorylated both in vitro and in vivo

To confirm that all the phosphorylation sites for Cdc2 kinase have been abolished in the CaD39-6F mutant, recombinant CaD39 and CaD39-6F were incubated with γ-^{32}P-labeled ATP in the presence of Cdc2 kinase. Phos-

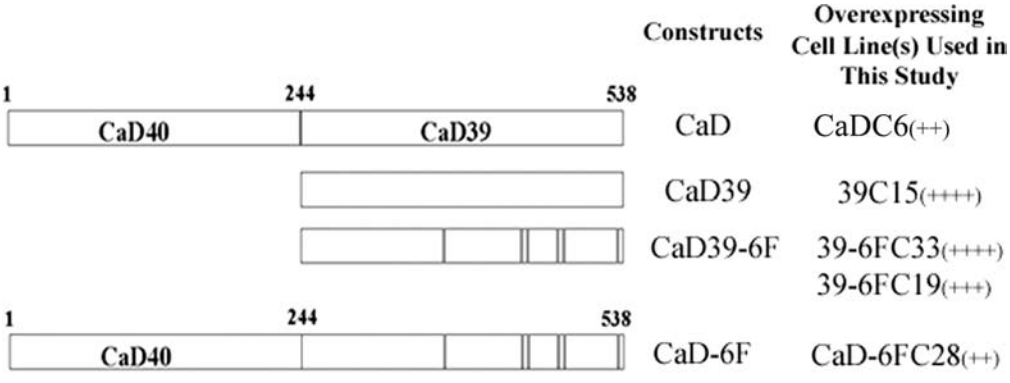

Figure 3. Summary of various human fibroblast CaD constructs and their overexpressing clones used in this study. The N-terminal fragment of human fibroblast caldesmon (CaD40) refers to aa 1–243, whereas the C-terminal fragment (CaD39) is from aa 244 to 538. The vertical lines in the CaD39 boxes of CaD39-6F and CaD-6F represent mutated Cdc2 phosphorylation sites. The expression levels of mutant proteins relative to endogenous CaD in stable lines used in this study are indicated by the numbers of + in parentheses.

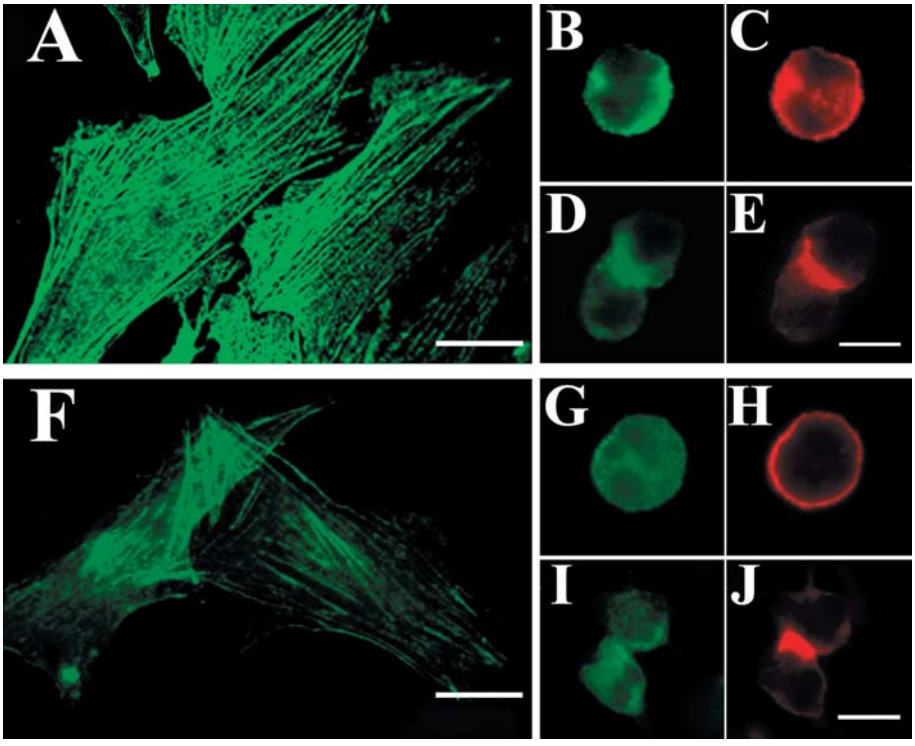

Figure 4. Immunofluorescence microscopy on interphase and mitotic cells of CaD39-6F-overexpressing line 39-6FC33 and the wild-type CHO line. The distributions of CaD39-6F mutant in the overexpressing clone 39-6FC33 were visualized using C21 monoclonal antibody at a 1000-fold dilution and FITC-conjugated goat anti-mouse IgG (*A, B, D*). At interphase (*A*), overexpressed CaD39-6F protein incorporated into stress fibers and the ruffle region. The mitotic 39-6FC33 cells counter-stained with phalloidin (*C, E*) showed that the majority of CaD39-6F was colocalized with actin filaments. Endogenous CaD in the wild-type CHO cells was visualized with C21 antibody at 100-fold dilution and FITC-conjugated goat anti-mouse IgG (*F, G, I*). In comparison to the cells overexpressing CaD39-6F mutant, endogenous CaD exhibited a diffuse staining pattern during mitosis and did not colocalize with actin filament as revealed by counterstaining with phalloidin (*H, J*). Bar, 10 µm.

phorylation was stopped at various time points and the reaction products were examined by SDS-PAGE and autoradiography. As shown in figure 5A, Cdc2 kinase was able to phosphorylate CaD39 and the level of ^{32}P incorporated into the CaD39 band increased with time, reaching a maximum level after 90 min of incubation (lanes 1–5, fig. 5A). In contrast, there was no detectable ^{32}P incorporation into the CaD39-6F protein within the same 120-min incubation (lanes 6–10, fig. 5A), although the concentration of CaD39-6F used in the reaction was about twice that of CaD39, as revealed in the Coomassie blue-stained gel (fig. 5B). This result demonstrated that the CaD39-6F mutations totally eliminated the Cdc2 kinase phosphorylation sites. To rule out the possibility that CaD39-6F protein could behave as a competitive inhibitor of Cdc2 kinase, the in vitro phosphorylation on histone H1 by Cdc2 kinase was performed in the presence of an increasing amount of CaD39-6F. As can be seen in figure 5C, there is no detectable inhibition of Cdc2 kinase activity by the presence of CaD39-6F mutant protein.

To further show that CaD39-6F could not be phosphorylated in vivo during mitosis, we performed a Western blot analysis on total cell extracts prepared from interphase and mitotic cells of clone 39-6FC33. We previously demonstrated that CaD39 protein in mitotic cells of clone 39C15 was highly phosphorylated and migrated much more slowly in an SDS/urea gel compared to that in interphase cells [17]. In comparison, CaD39-6F from both interphase and mitotic cells had the same mobility on an SDS/urea gel (lanes 1 and 2, fig. 6A), while the endogenous CaD present in the CaD39-6F-expressing cells exhibited retarded gel mobility in the mitotic cell extract. This retardation of CHO CaD from mitotic 39-6FC33 cells is identical to that of CHO CaD from non-expressing control cells (lanes 3 and 4, fig. 6A). Similarly, the cell extracts prepared from CaDC6 (overexpressing wild-type full-length CaD) and CaD-6FC28 (overexpressing full-length CaD-6F) were examined using monoclonal antibody C57 that specifically recognizes the N terminus of human CaD and does not cross-react with the endogenous CHO CaD [17]. As shown in figure 6B, the overexpressed wild-type CaD from mitotic cells displayed retarded gel mobility, while CaD-6F mutant from mitotic and interphase cells migrated at the same rate. These results demonstrated that the mitosis-specific phosphoryla-

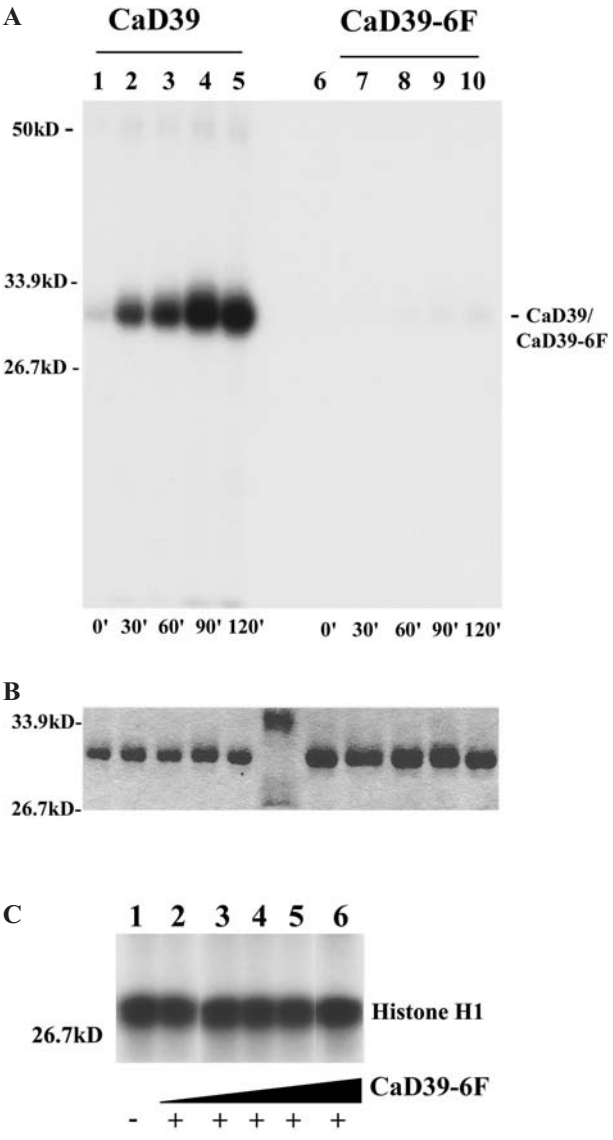

Figure 5. In vitro phosphorylation of CaD39 and CaD39-6F by Cdc2 kinase. The reaction mixture containing 5 µM CaD39 (lanes 1–5) or 10 µM CaD39-6F (lanes 6–10) was incubated with 1.5 units of Cdc2 kinase at 37 °C. At 0, 30, 60, 90, and 120 min of incubation, aliquots of samples were removed, the reaction terminated, and ^{32}P incorporation into CaD39 and CaD39-6F analyzed by SDS-PAGE (*B*) and autoradiography (*A*). Only the portion of the Coomassie blue-stained gel containing CaD39 and CaD39-6F is shown in (*B*). The lane in the middle between CaD39 and CaD39-6F samples was loaded with protein molecular weight markers. In vitro, Cdc2 kinase phosphorylated recombinant CaD39 but not CaD39-6F. (*C*) Phosphorylation of histone H1 by Cdc2 kinase in the absence and presence of CaD39-6F. The addition of increasing amounts of CaD39-6F (lanes 2–6) did not reduce the in vitro phosphorylation of histone H1 protein by Cdc2, suggesting that CaD39-6F does not behave as a competitive inhibitor.

tion of CaD detected by the SDS/urea gel did not occur on either CaD39-6F or CaD-6F mutant proteins in vivo.

CaD39-6F cannot efficiently dissociate from actin filament during mitosis

Immunofluorescence microscopy of the overexpressing cells revealed that most of the CaD39-6F colocalized with F-actin during mitosis (fig. 4B, D), suggesting that the mutant proteins may not dissociate from the actin filaments during mitosis. To test this possibility, tropomyosin-enriched microfilaments were isolated from interphase and nocodazole-arrested mitotic 39-6FC33 cells, and analyzed by SDS/urea gel and a Western blot assay. As shown in figure 7B, the amount of CaD39-6F present in the microfilament fraction of mitotic 39-6FC33 cells (lane 2) is comparable to that of interphase cells (lane 1). This observation indicates that the majority of CaD39-6F remains associated with microfilaments during mitosis. The behavior of CaD39-6F proteins, associating with microfilaments equally in interphase and mitotic cells, appears to differ from that of CaD39 proteins in interphase and mitotic 39C15 cells [17]. Moreover, the microfilament fraction of 39-6FC33 at mitosis contained much less endogenous CHO CaD than the interphase fraction. Considering that nearly equivalent amounts of endogenous CaD were present in the total cell extracts from mitotic and interphase cells (lane 1 and 2, fig. 6A), the noticeably reduced level of endogenous CaD in the microfilament fraction indicates that wild-type CaD dissociates from microfilaments during mitosis. The fact that the 39-6FC33 cells can still proceed to cytokinesis indicates that the contraction force of the actomyosin in the contractile ring is not severely impaired despite the association of CaD39-6F with the microfilaments.

Forced expression of CaD39-6F affects cell size and delays the mitotic processs – 2D analyses

Western blot analyses showed that CaD39-6F cannot undergo phosphorylation during mitosis and is unable to dissociate from microfilaments efficiently. In addition, previous in vitro analyses showed that a rat CaD fragment mutant that was equivalent to CaD39-6F was able to inhibit actomyosin ATPase activity in the presence of Cdc2 kinase [27]. The altered properties of the mutant protein might therefore impair the reorganization of actin filaments during cell division. To further investigate the effects of CaD39-6F expression in vivo, we videotaped mitosis in nine cells each from the 39-6FC5 (non-expressing) and 39-6FC33 (overexpressing) lines and analyzed them over the period between the start of anaphase and 50% cytokinesis, during which time the microfilaments underwent dramatic rearrangements. The mutant cells were able to progress to anaphase, form cleavage furrows, and divide symmetrically. However, the total elapsed time for this period was significantly longer ($p = 0.004$) in 39-

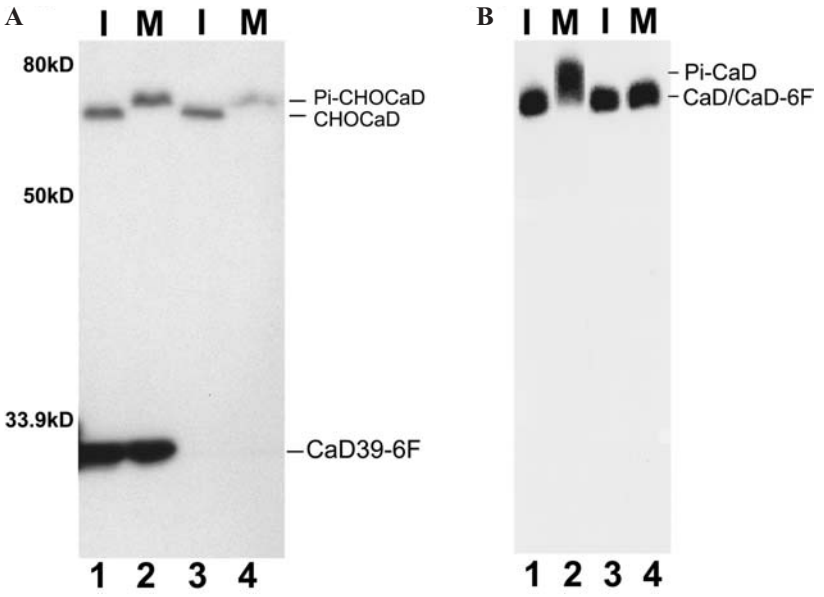

Figure 6. In vivo phosphorylation of CaD during mitosis. (*A*) Total extracts from interphase (I) and mitotic (M) cells of 39-6FC33 (lanes 1, 2) and normal CHO lines (lanes 3, 4) were resolved on 8% SDS-PAGE with 6 M urea, transferred to nitrocellulose, and then blotted with monoclonal antibody C21. CaD39-6F from mitotic 39-6FC33 cells migrated at the same rate as that from interphase cells (lanes 1, 2), while the endogenous CHO CaD from both 39-6FC33 and normal CHO mitotic cells (Pi-CHOCaD in lanes 2, 4) migrated slower than that from interphase cells (CHOCaD in lanes 1, 3). (*B*) Total cell extracts were prepared from interphase and mitotic cells of wild-type full-length CaD-expressing line CaDC6 (lanes 1, 2) and mutant full-length CaD-6F-expressing line CaD-6FC28 (lanes 3, 4). After urea/SDS-PAGE, the proteins were immunoblotted with monoclonal antibody C57 against the N terminus of human CaD. At mitosis, wild-type CaD showed shifted migration (Pi-CaD in lane 2) compared to the protein in interphase (CaD in lane 1), while CaD-6F mutant from mitotic (lane 4) cells displayed the same mobility on the gel as that from interphase cells (lane 3).

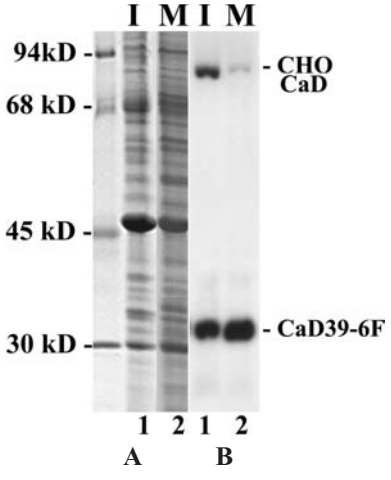

Figure 7. Comparison of tropomyosin-enriched microfilaments isolated from interphase and mitotic 39-6FC33 cells. The microfilament fractions from interphase (I, lane 1) and mitotic (M, lane 2) 39-6FC33 cells were subjected to urea/SDS-PAGE analysis (*A*), followed by Western blotting assay (*B*). The proportion of CaD39-6F bound to microfilaments in mitotic cells (lane 2 of panel B) is comparable to that in interphase cells (lane 1 of panel B), while the majority of endogenous caldesmon (CHO CaD) became dissociated from the microfilaments during mitosis.

6FC33 (14.7 ± 2.7 min) than that in the control (10.7 ± 2.2 min), suggesting that the mitotic process may be impaired in CaD39-6F-expressing cells. To further detect the subtle changes in mitotic behavior, 39-6FC33 and 39-6FC5 cells were motion-analyzed using 2D-DIAS from the onset of anaphase through 50% cytokinesis. Motility parameters calculated from the centroid position, such as mean instantaneous speed and directional change, showed no significant differences between the over- and non-expressing cell lines (data not shown), suggesting that CaD39-6F expression did not affect cell motility during mitosis. In contrast, the shape parameters calculated from the contour changes of the cell perimeter, including mean area, mean perimeter, maximum length, and maximum width, were significantly larger for the overexpressing cells over the time interval studied (table 1). In particular, the observed increase in mean radial length in the overexpressing cells, defined as the average distance of the boundary of the object to the centroid, was consistent with the impression that cells overexpressing CaD39-6F became bigger and larger during mitosis. Comparisons of parameters for cell shape complexity such as mean roundness, mean radial deviation, mean convexity and concavity showed no significant difference, suggesting that 39-6FC5 and 39-6FC33 cells might have similar round shapes during mitosis, or that the subtle difference could not be detected by 2D analysis. Altogether, the re-

Table 1. 2D-DIAS computer-assisted measurements of shape parameters of 39-6FC5, 39-6FC33, and 39-6FC19 cells during the intervals between the start of anaphase and 50% cytokinesis.

	Number of cells	Mean area (μm²)	Mean maximum length (μm)	Mean perimeter (μm)	Mean maximum width (μm)	Mean radial length (μm)	Mean 2D convexity (degree)	Mean 2D concavity (degree)
39-6FC5[a]	9	211 ± 24	18.9 ± 1.3	55.3 ± 3.5	14.5 ± 0.7	8.2 ± 0.5	991 ± 125	636 ± 124
39-6FC33[b]	9	244 ± 35	20.6 ± 1.8	59.6 ± 4.6	15.5 ± 0.9	8.8 ± 0.6	901 ± 57	548 ± 63
39-6FC19[c]	6	234 ± 9	20.4 ± 0.5	59.3 ± 1.9	15.2 ± 0.5	8.7 ± 0.2	934 ± 174	574 ± 174
p value								
a vs b		0.04	0.05	0.04	0.02	0.03	NS	NS
a vs c		0.02	0.01	0.01	0.04	0.02	NS	NS
b vs c		NS	NS	NS	NS	NS	NS	NS

50% cytokinesis, the time required for a 50% reduction of the size of the cleavage furrow. A t test was performed to calculate p values after the tests of the samples for normality and equal variance. NS, not significant ($p > 0.05$).

sults from the quantitative 2D analysis suggest that overexpression of CaD39-6F leads to an increase in cell size during mitosis, particularly from the beginning of anaphase to the completion of 50% cytokinesis. By analyzing interphase cells migrating from a wound area, we did not detect significant differences in cell size between non-expressing and CaD39-6F-overexpressing cells (area: 1079 ± 367 and 1190 ± 424 μm², respectively; $p = 0.578$), suggesting that the effect of CaD39-6F on cell size is specific to mitotic cells. In addition to 39-6FC33, we analyzed another independent cell line, 39-6FC19, which also overexpresses CaD39-6F. This cell line also exhibited significantly greater cell size parameters than the control (table 1), while the differences between 39-6FC33 and 39-6FC19 in all measured parameters were not statistically significant ($p > 0.05$), suggesting that the mitotic defects we detected result from CaD39-6F expression rather than from a second gene mutation caused by a random integration of exogenous DNA.

CaD39-6F mutant cell lines display excessive blebbing during cytokinesis – 3D analyses

To better document morphological and size differences, 3D-DIAS analyses were performed on four cells each of the overexpressing cell line 39-6FC33 and the non-expressing cell line 39-6FC5. Table 2 shows motility and shape parameters obtained from the 3D-DIAS analysis. Consistent with the bigger cell size shown in the 2D analyses, CaD39-6F-expressing cells had a larger cell volume and cell surface area than non-expressing cells, a 15% increase in volume, and a 14% increase in surface area (table 2). Both differences were statistically significant (table 2). The 3D convexity and concavity parameters of CaD39-6F-expressing cells, computed from 2D projections of the 3D optical sections, were significantly greater than those of non-expressing control cells (table 2), suggesting a more complex cell shape in the CaD39-6F-overexpressing cells. The detection of increased cell shape complexity in the 3D (table 2) but not 2D (table 1) analysis is likely due to the fact that the blebs observed were small and covered the entire cell surface (fig. 8D–F), which could only be measured accurately by 3D reconstruction of the living cell. These small blebs became almost negligible in 2D-DIAS measurements (table 1) where only a section of the cell body was monitored. A representative 39-6FC33 and a representative 39-6FC5 cell were both reconstructed from the start to 50% cytokinesis as faceted images in which protrusions from the main cell body were color-coded red (fig. 9). The 39-6FC33 cell formed blebs very early and their number increased dramatically as cytokinesis proceeded. By 50% completion of cytokinesis, more than 30% of the cell body was covered with blebs (fig. 9B). In contrast, only a few blebs were formed at the late stage of cytokinesis in

Table 2. 3D-DIAS computer-assisted measurements of motility and shape parameters of 39-6FC5 and 39-6FC33 cells during the intervals between the start of anaphase and 50% cytokinesis.

	Number of cells analyzed	Speed (μm/min)	Volume (μm³)	Surface area (um²)	Height (μm)	Mean 3D convexity (degree)	Mean 3D concavity (degree)
39-6FC5	4	7.3 ± 3.5	2876 ± 239	1454 ± 131	18.1 ± 0.6	807 ± 98	446 ± 98
39-6FC33	4	5.6 ± 1.4	3310 ± 239	1660 ± 64	17.7 ± 1.8	1103 ± 160	741 ± 159
p value		NS	0.04	0.02	NS	0.02	0.02

50% cytokinesis, the time required for a 50% reduction of the size of the cleavage furrow. A t test was performed to calculate p values after the tests of the samples for normality and equal variance. NS, not significant ($p > 0.05$).

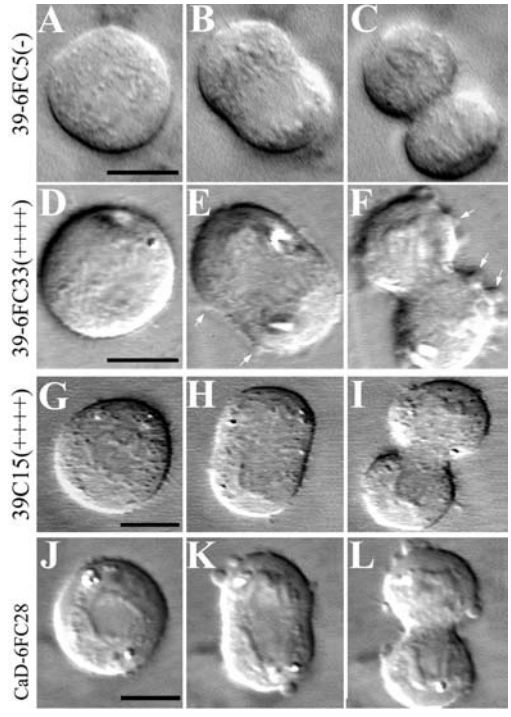

Figure 8. Differential interference contrast (DIC) micrographs of mitotic cells from non-expressing control 39-6FC5 (*A–C*), 39-6FC33 (*D–F*), 39C15 (*G–I*), and CaD-6FC28 (*J–L*) lines at the start of anaphase (*A, D, G, I*), at the start of cytokinesis (*B, E, H, K*), and at 50% cytokinesis (*C, F, I, L*). Overexpression of the CaD39-6F or CaD-6F mutant led to abnormal numbers of blebs (arrows) formed on the surface of the mitotic cells (*E, F, K, L*). Overexpression of CaD39 did not cause this phenotype (*H, I*). Bar, 10 µm.

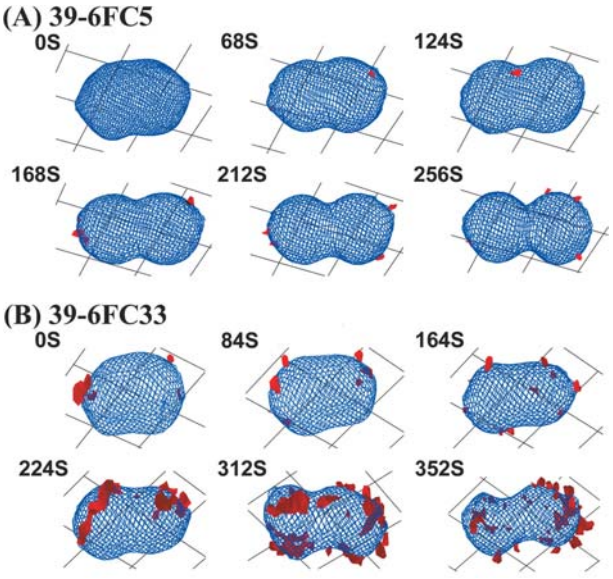

Figure 9. Time series of 3D reconstructions of representative over-expressing 39-6FC33 (*B*) and non-expressing 39-6FC5 (*A*) cells. The time series spans the start of cytokinesis to 50% completion of cytokinesis for both cells. Mitotic cells grown on coverslips were observed under a Zeiss Axioplan 2 microscope equipped with DIC optics. Optic sectioning and image recording were performed as described in Materials and methods. Perimeters of the in-focus portion of each section were manually digitized into the 3D-DIAS data file. The digitized perimeters of the in-focus portions of the optic sections were filled and stacked to create a pseudo 3D reconstruction. Both 39-6FC5 and C33 reconstructions were then slanted 60° relative to the grid plane. The distance between horizontal lines in the grid plane is 10 µm. The red color areas represent blebs.

the control cell 39-6FC5 and the number did not increase over time (fig. 9A). Collectively, these results suggest that CaD39-6F-expressing cells have a much more complex cell shape than the control cells during mitosis, likely due to the presence of many small blebs on the surface of CaD39-6F-expressing cells.

The mitotic defects in CaD39-6F-expressing cells may represent combined defects of CaD39- and CaD-6F-overexpressing cells

We previously showed that in the CaD39-overexpressing clone 39C15, a significant portion of CaD39 was not fully phosphorylated during mitosis [17]. Concomitantly, the incidence of multinuclearity increased significantly in the 39C15 clone compared to that in normal cells [17]. Hence, underphosphorylation of CaD39 may cause some cytokinesis defects in the CaD39-overexpressing cells. To test this possibility, mitotic cells from the 39C15 cell line were analyzed using 2D-DIAS. The time required for 39C15 (13.3 ± 1.8 min, table 3) to proceed from anaphase to 50% cytokinesis was prolonged, although still less than that required for 39-6FC33 cells (14.7 ± 2.7 min). Similarly, the difference in the cell size between 39C15 and wild-type cells was evident in the measurement of maximum length, mean area, and mean perimeter (table 3), suggesting that the association of the CaD C-terminal fragments on the microfilaments may be responsible for an increase in cell size at mitosis. Further 2D-DIAS analyses revealed no significant difference in either motility or cell size parameters between the CaD-6F-expressing cells (CaD-6FC28) and the control except for a prolonged division time (15.11 ± 2.2 min, table 3), indicating that the lack of N termini in CaD39 and CaD39-6F, rather than the insufficient phosphorylation, is the critical factor in determining the cell size increase. Compared to CaD39- and CaD39-6F-expressing cells, the presence of an N-terminal fragment in CaD-6FC28 may function to regulate the cytoskeleton and play an important role in controlling cell size during cell division.

CaD39-expressing cells on average did not exhibit excess blebs as did CaD39-6F-expressing cells (fig. 8G–I). Of the 6 39C15 cells examined, only 1 cell (17%) blebbed over more than 30% of the cell surface during cytokinesis, while 11 out of 18 (61%) mitotic 39-6FC33 cells showed excess blebs in the same period. In contrast, 6 out of 7 CaD-6FC28 cells (86%), which expressed CaD-6F, displayed increased bleb formation at early cytokinesis as did 39-6F-overexpressing cells (fig. 8J–L), suggesting

Table 3. Computer-assisted analysis of mitotic behaviors of 39C15 and CaD-6FC28 cells during the intervals between the start of anaphase and 50% cytokinesis.

	Number of cells	Total elapsed times (min)	Mean area (μm^2)	Mean maximum length (μm)	Mean perimeter (μm)	Mean radial length (μm)
39-6FC5[a] (control)	9	10.7 ± 2.2	211 ± 24	18.9 ± 1.3	55.3 ± 3.5	8.2 ± 0.5
39C15[b]	7	13.3 ± 1.8	248 ± 31	20.8 ± 1.4	59.7 ± 4.0	8.9 ± 0.6
CaD-6FC28[c]	5	15.11 ± 2.2	217 ± 12	20.2 ± 1.3	57.2 ± 2.7	8.4 ± 0.3
p value						
a vs. b		0.03	0.02	0.02	0.03	0.02
a vs. c		0.004	NS	NS	NS	NS

50% cytokinesis, the time required for a 50% reduction of the size of the cleavage furrow. A t test was performed to calculate p values after the tests of the samples for normality and equal variance. NS, not significant ($p > 0.05$).

that total abolishment of CaD phosphorylation by Cdc2 kinase may disrupt the cortical tension during mitosis, leading to the formation of numerous blebs.

Discussion

To assess the impact of mitosis-specific phosphorylation on CaD function, we generated CaD mutants in which all six Cdc2 kinase sites were mutated to alanine. Stable cell lines overexpressing CaD39-6F or CaD-6F were isolated, characterized, and compared to the non-expressing cell line 39-6FC5 as well as the cell line 39C15, which overexpresses the CaD39 fragment. Using computer-assisted motion analysis methods, we report here that CaD39-6F-overexpressing clones (39-6FC33 and 39-6FC19) take longer to proceed from the beginning of anaphase to 50% cytokinesis and display a larger cell size than the non-expressing control cell line (39-6FC5). Moreover, cells overexpressing non-phosphorylatable CaD or CaD39 form abnormal blebs early in cytokinesis. Concomitant with the mitotic defects, CaD39-6F protein cannot be phosphorylated and the majority remains associated with microfilaments during cell division, suggesting that the failure of phosphorylation leads to the association of CaD on actin filaments during mitosis. In vitro data have shown that the association of CaD can have two effects: one is to enhance the binding of tropomyosin to actin filaments and stabilize the microfilaments [8]; the other is to inhibit the myosin ATPase activity [27]. Both or either of these may account for the mutant phenotype we observed in the CaD39-6F-overexpressing cells. The association of CaD39-6F with microfilaments may cause the lack of the contraction force in the actomyosin system during mitosis, particularly at the contractile ring where CaD39-6F is highly concentrated. The loss of contractility might thus contribute to the delay of cytokinesis in the CaD39-6F-overexpressing cells, as proposed by Matsumura's group [14]. Nonetheless, those cells were still able to generate enough contraction force to pinch off the two daughter cells and proceed through cytokinesis. Unlike the in vitro observations, the abolishment of Cdc2 phosphorylation sites and the consequent maintenance of CaD on actin do not seem to noticeably inhibit the actomyosin ATPase activity. The discrepancy between in vitro and in vivo data may be due to the fact that some other regulatory mechanisms, such as Ca^{2+}/calmodulin binding, may still regulate the activity of CaD without requiring its complete dissociation from actin filaments in the living cells, as suggested by Marston's group [3]. Alternatively, the association of CaD39-6F during cell division may stabilize the actin filaments and thus impair the rearrangement of the microfilaments in both the cortex region and contractile ring during mitosis. Yamashiro et al. [14] have reported that transient expression of a rat fibroblast CaD fragment equivalent to the CaD39-6F mutant results in a transient existence of stress fibers during cell division. Although we did not observe stress fiber structures at mitosis in our stable clones 39-6FC33 and 39-6FC19, the fact that most of the protein remained associated with actin filaments suggests that it may still function to stabilize the actin filament structure. Consistent with this idea, CaD39-6F-expressing cells were more resistant to cytochalasin D disruption of actin bundles at interphase than the control cells (data not shown), as previously demonstrated for CaD39-overexpressing cells [16]. The actin stabilization by CaD39-6F may increase the rigidity of microfilaments and impair their rearrangement during cytokinesis, which may in turn disrupt the proper cortical tension required for cytokinesis and thus lead to the mitotic defects such as blebbing and prolonged dividing time. Since CaD39-expressing cells adhered faster to substrata than control cells and exhibited enhanced spreading immediately after attachment at interphase [17], it seems reasonable to speculate that enhancement of microfilament stability at mitosis by CaD39-6F binding may also lead to the advantages of attachment and spreading, resulting in an increase in cell size. A smaller percentage of overhang volume detected in 39-6FC33 cells by 3D-DIAS (data not shown) is also consistent with the idea that CaD39-6F-expressing cells had a larger portion of their surface actually attached to

substrata during mitosis. We, therefore, propose that the stabilization of the microfilaments by the association of CaD39-6F, rather than the lack of sufficient contraction force, is responsible for the mitotic defects we observed in the CaD39-6F-overexpressing cells.

In addition to the CaD39-6F-expressing cells, we also analyzed the mitotic behaviors of CaD39- and full-length CaD-6F-expressing cells. Similar to CaD39-6F overexpressors, the stable clone expressing wild-type CaD39 also exhibited larger cell size compared to the control. The CaD39 protein in the cell line 39C15 was underphosphorylated during cell division, likely due to the saturation of Cdc2 kinase activity by the overexpression of CaD39. Coincident with underphosphorylation, 20% of CaD39 still remained on the microfilaments at mitosis [17]. Therefore, the underphosphorylated C-terminal fragment of CaD seems to remain associated with the microfilaments during cell division, which would in turn cause mitotic defects in cell size. In contrast to CaD39, overexpression of full-length CaD-6F did not affect cell size. The expression level of the exogenous protein in the CaD-6F-overexpressing clone, which was about one-fifteenth of that in the CaD39-6F-overexpressing clones, was likely not high enough to bring about the cell size defects at mitosis. However, a more favorable but not exclusive interpretation would be that the presence of the CaD N-terminal fragment is important for controlling cell size at mitosis. The phenotypic differences between the expressions of the C-terminal half and the full-length proteins were also observed in wild-type CaD39- and CaD-expressing cells. In contrast to CaD39, overexpression of full-length CaD could not stabilize tropomyosin in interphase (data not shown), suggesting that the effects of the full-length and the C-terminal fragment of CaD on microfilament organization are not equivalent.

Of note, the expression of both CaD39-6F and CaD-6F results in the emergence of blebs, suggesting that phosphorylation of CaD by Cdc2 kinase is critical for maintaining the proper cortical tension required for mitosis and suppressing bleb formation. Cortical tension requires an intact actin cytoskeleton and is believed to result from a combination of the contractile activity of myosins (at least myosin I and II) and the dynamics of actin regulated by a variety of actin-binding proteins [36–38]. In the CaD39-6F-expressing cells, the mutant protein stabilizes the actin filaments beneath the cell membrane, making them more rigid and less dynamic. The rigid actin network may lead to the increase of local cytosolic pressure, which may in turn push the membrane outward to form the blebs. In addition, CaD39-6F may possibly stimulate actin polymerization as shown in vitro [6]. The growing actin filaments may push the membrane outward, leading to the bleb formation. Consistent with our observations, coincident with the morphological changes in the transformed fibroblasts, CaD was reported to become specifically localized in the cell surface blebs [39], suggesting a possible involvement of CaD in the control of bleb formation.

The blebs found in dividing CaD39-6F-expressing cells are different from those found in the chimeric tropomyosin hTM5/3-expressing cells that we have previously characterized [34]. Compared to the small and numerous blebs in 39-6FC33 cells, the blebs formed in the hTM5/3-overexpressing cells were larger yet less frequent. In addition to bleb formation, the hTM5/3-overexpressing cells usually had difficulties in defining the position of the cleavage furrow, resulting in the twisting of the mitotic cells and the detachment of one of the evolving daughter cells during cytokinesis [34]. In contrast, the CaD39-6F-overexpressing cells do not have this problem and have almost equally divided daughter cells with many small blebs. These results suggest a distinct but overlapping role for tropomyosin and caldesmon in a dividing cell. Force-expressed CaD39-6F proteins are mainly found in the contractile ring and membrane cortex region of dividing cells (fig. 4B, C), whereas force-expressed chimeric hTM5/3 is localized solely in the contractile ring [34]. Moreover, although both of them can stabilize microfilaments, hTM5/3 stimulates myosin ATPase activity while CaD inhibits it [8]. The excessive contraction force of the actomyosin system induced by hTM5/3 may result in the asymmetric flex at the cleavage furrow in hTM5/3-overexpressing cells, while the lack of contraction in the CaD39-6F-overexpressing cells at both the cleavage furrow and cortical region may contribute to prolonged dividing time and formation of excess blebs over the cell body.

Noteworthy is that, despite the defects discussed above, we were still able to obtain multiple cell lines stably expressing CaD39-6F, suggesting that the defect of CaD phosphorylation by Cdc2 at mitosis is not lethal to the cell. Similarly, inhibition of cytokinesis by microinjection of mutant caldesmon lacking Cdc2 phosphorylation sites into CHO cells was reported to be not as effective as that in *Xenopus* embryos [14]. Thus, CaD phosphorylation does not seem to play a direct role in regulating cell rounding, and contractile ring assembly and function. However, Cdc2 phosphorylation of CaD may play an important role in maintaining cortical tension to suppress surface bleb formation. The lengthening of anaphase-telophase and the increase in cell size for both CaD39- and CaD39-6F-expressing cells could mean that the effects may not be related to phosphorylation. Cdc2 phosphorylation might not be the only way to relieve the inhibition of CaD on the cytoskeleton in mitotic cells. Of interest would be to investigate the function of Ca^{2+}/calmodulin in CaD regulation during cell division. Immunofluorescence microscopy of CaD39-6F-expressing cells showed that the expressed mutant proteins remained concentrated in the contractile ring and the cell cortex re-

gion at anaphase, where the active form of Ca^{2+}/calmodulin is located [40].

Acknowledgements. We would like to thank A. Matveia and G. Nitzsche for their technical support on 3D-DIAS analysis. This work was supported by a grant HD18577 from National Institutes of Health and a grant from the W. M. Keck Foundation.

1 Bretscher A. (1986) Thin filament regulatory proteins of smooth- and non-muscle cells. Nature **321:** 726–728
2 Huber P. A. (1997) Caldesmon. Int. J. Biochem. Cell Biol. **29:** 1047–1051
3 Marston S. B. and Redwood C. S. (1991) The molecular anatomy of caldesmon. Biochem. J. **279:** 1–16
4 Matsumura F. and Yamashiro S. (1993) Caldesmon. Curr. Opin. Cell Biol. **5:** 70–76
5 Sobue K. and Sellers J. (1991) Caldesmon, a novel regulatory protein in smooth muscle and nonmuscle actomyosin systems. J. Biol. Chem. **266:** 12115–12118
6 Galazkiewicz B., Belagyi J. and Dabrowska R. (1989) The effect of caldesmon on assembly and dynamic properties of actin. Eur. J. Biochem. **181:** 607–614
7 Ikebe M. and Reardon S. (1988) Binding of caldesmon to smooth muscle myosin. J. Biol. Chem. **263:** 3055–3058
8 Novy R. E., Sellers J. R., Liu L.-F. and Lin J. J.-C. (1993) In vitro functional characterization of bacterially expressed human fibroblast tropomyosin isoforms and their chimeric mutants. Cell Motil. Cytoskel. **26:** 248–261
9 Yamashiro-Matsumura S. and Matsumura F. (1988) Characterization of 83-kilodalton nonmuscle caldesmon from cultured rat cells: stimulation of actin binding of nonmuscle tropomyosin and periodic localization along microfilaments like tropomyosin. J. Cell Biol. **106:** 1973–1983
10 Ishikawa R., Yamashiro S. and Matsumura F. (1989) Differential modulation of actin-severing activity of gelsolin by multiple isoforms of cultured rat cell tropomyosin: potentiation of protective ability of tropomyosins by 83-kDa nonmuscle caldesmon. J. Biol. Chem. **264:** 7490–7497
11 Ishikawa R., Yamashiro S. and Matsumura F. (1989) Annealing of gelsolin-severed actin fragments by tropomyosin in the presence of Ca^{2+}. J. Biol. Chem. **264:** 16764–16770
12 Ishikawa R., Yamashiro S., Kohama K. and Matsumura F. (1998) Regulation of actin binding and actin bundling activities of fascin by caldesmon coupled with tropomyosin. J. Biol. Chem. **273:** 26991–26997
13 Earley J. J., Su X. and Moreland R. S. (1998) Caldesmon inhibits active crossbridges in unstimulated vascular smooth muscle: an antisense oligodeoxynucleotide approach. Circ. Res. **83:** 661–667
14 Yamashiro S., Chen H., Yamakita Y. and Matsumura F. (2001) Mutant caldesmon lacking cdc2 phosphorylation sites delays M-phase entry and inhibits cytokinesis. Mol. Biol. Cell **12:** 239–250
15 Helfman D. M., Levy E. T., Berthier C., Shtutman M., Riveline D., Grosheva I. et al. (1999) Caldesmon inhibits nonmuscle cell contractility and interferes with the formation of focal adhesions. Mol. Biol. Cell **10:** 3097–3112
16 Warren K. S., Lin J. L.-C., Wamboldt D. D. and Lin J. J.-C. (1994) Overexpression of human fibroblast caldesmon fragment containing actin-, Ca^{++}/calmodulin-, and tropomyosin-binding domains stabilizes endogenous tropomyosin and microfilaments. J. Cell Biol. **125:** 359–368
17 Warren K. S., Shutt D. C., McDermott J. P., Lin J. L.-C., Soll D. R. and Lin J. J.-C. (1996) Overexpression of microfilament-stabilizing human caldesmon fragment, CaD39, affects cell attachment, spreading, and cytokinesis. Cell Motil. Cytoskel. **34:** 215–229
18 Fraser I. D. C. and Marston S. B. (1995) In vitro motility analysis of smooth muscle caldesmon control of actin-tropomyosin filament movement. J. Biol. Chem. **270:** 19688–19693
19 Haeberle J. R., Trybus K. M., Hemric M. E. and Warshaw D. M. (1992) The effects of smooth muscle caldesmon on actin filament motility. J. Biol. Chem. **267:** 23001–23006
20 Horiuchi K. Y. and Chacko S. (1995) Effect of unphosphorylated smooth muscle myosin on caldesmon-mediated regulation of actin filament velocity. J. Muscle Res. Cell Motil. **16:** 11–19
21 Okagaki T., Higashi-Fujime S., Ishikawa R., Takama-Ohmuro H. and Kohama K. (1991) In vitro movement of actin filaments on gizzard smooth muscle myosin: requirement of phosphorylation of myosin light chain and effects of tropomyosin and caldesmon. J. Biochem. **109:** 858–866
22 Shirinsky V. P., Biryukov K. G., Hettasch J. M. and Sellers J. (1992) Inhibition of the relative movement of actin and myosin by caldesmon and calponin. J. Biol. Chem. **267:** 15886–15892
23 Yamakita Y., Yamashiro S. and Matsumura F. (1992) Characterization of mitotically phosphorylated caldesmon. J. Biol. Chem. **267:** 12022–12029
24 Yamashiro S., Yamakita Y., Ishikawa R. and Matsumura F. (1990) Mitosis-specific phosphorylation causes 83k non-muscle caldesmon to dissociate from microfilaments. Nature **344:** 675–678
25 Yamshiro S., Yamakita Y., Hosoya H. and Matsumura F. (1991) Phosphorylation of non-muscle caldesmon by $p34^{cdc2}$ kinase during mitosis. Nature **349:** 169–172
26 Hosoya N., Hosoya H., Yamashiro S., Mohri H. and Matsumura F. (1993) Localization of caldesmon and its dephosphorylation during cell division. J. Cell Biol. **121:** 1075–1082
27 Yamashiro S., Yamakita Y., Yoshida K., Takiguchi K. and Matsumura F. (1995) Characterization of the COOH terminus of non-muscle caldesmon mutants lacking mitosis-specific phosphorylation sites. J. Biol. Chem. **270:** 4023–4030
28 Lin J. J.-C., Davis-Nanthakumar E. J., Jin J.-P., Lourim D., Novy R. E. and Lin J. L.-C. (1991) Epitope mapping of monoclonal antibodies against caldesmon and their effects on the binding of caldesmon to Ca^{++}/calmodulin and to actin or actin-tropomyosin filaments. Cell Motil. Cytoskel. **20:** 95–108
29 Eaton B. L., Kominz D. R. and Eisenberg E. (1975) Correlation between the inhibition of the acto-heavy meromyosin ATPase and the binding of tropomyosin to F-actin: effects of Mg^{++}, KCl, troponin I, and troponin C. Biochemistry **14:** 2718–2724
30 Matsumura F., Yamashiro-Matsumura S. and Lin J. J.-C. (1983) Isolation and characterization of tropomyosin-containing microfilaments from cultured cells. J. Biol. Chem. **258:** 6636–6644
31 Soll D. R. (1995) The use of computers in understanding how animal cells crawl. Int. Rev. Cytol. **8:** 439–454
32 Soll D. R. and Voss E. (1998) Two- and three-dimensional computer systems for analyzing how cells crawl. In: Motion Analysis of Living Cells, pp. 25–52, Soll D. R. and Wessels D. (eds), Wiley, New York
33 Soll D. R., Voss E., Johnson O. and Wessels D. J. (2000) Three-dimensional reconstruction and motion analysis of living crawling cells. Scanning **22:** 249–257
34 Wong K., Wessels D., Krob S. L., Matveia A. R., Lin J. L.-C., Soll D. R. et al. (2000) Forced expression of a dominant-negative chimeric tropomyosin causes abnormal motile behavior during cell division. Cell Motil. Cytoskel. **45:** 121–132
35 Wessels D., Voss E., Bergen N. von, Burns R., Stites J. and Soll D. R. (1998) A computer-assisted system for reconstructing and interpretating the dynamic three-dimensional relationships of the outer surface, nucleus, and pseudopods of crawling cells. Cell Motil. Cytoskel. **41:** 225–246
36 Pasternak C., Spudich J. A. and Elson E. L. (1989) Capping of surface receptors and concomitant cortical tension are generated by conventional myosin. Nature **341:** 549–551

37 Tsai M. A., Frank R. S. and Waugh R. E. (1994) Passive mechanical behavior of human neutrophils. Biophys. J. **66:** 2166–2172
38 Dai J., Ting-Beall H. P., Hochmuth R. M., Sheetz M. P. and Titus M. A. (1999) Myosin I contributes to the generation of resting cortical tension. Biophys. J. **77:** 1168–1176
39 McManus M. J., Lingle W. L., Salisbury J. L. and Maihle N. J. (1997) A transformation-associated complex involving tyrosine kinase signal adaptor proteins and caldesmon links v-ErbB signaling to actin stress fiber disassembly. Proc. Natl. Acad. Sci. USA **94:** 11351–11356
40 Li C. J., Heim R., Lu P., Pu Y., Tsien R. Y. and Chang D. C. (1999) Dynamic redistribution of calmodulin in HeLa cells during cell division as revealed by a GFP-calmodulin fusion protein technique. J. Cell Sci. **112:** 1567–1577